Rapid Calculation of Regional Cerebral Blood Flow and Distribution Volume Using Iodine-123-Iodoamphetamine and Dynamic SPECT

Hiroshi Ito, Hidehiro Iida, Peter M. Bloomfield, Matsutaro Murakami, Atsushi Inugami, Iwao Kanno, Hiroshi Fukuda and Kazuo Uemura

Departments of Radiology and Nuclear Medicine, Research Institute for Brain and Blood Vessels, Akita; and Division of Brain Sciences, Department of Nuclear Medicine and Radiology, Institute of Development, Aging and Cancer, Tohoku University, Sendai, Japan

Iodine-123-iodoamphetamine (IMP) is commonly used as a flow tracer for SPECT due to its large first-pass extraction fraction. Significant clearance from the brain, however, causes changes in distribution and underestimation of CBF values when a conventional microsphere model is applied to prolonged data acquisition. We have developed a rapid method to calculate CBF images in which clearance effects are taken into account. **Methods:** A dynamic SPECT scan was obtained from five subjects (four patients with cerebral infarctions and one healthy volunteer) following intravenous injection of IMP lasting 1 min. The arterial input function was obtained by frequent blood sampling and measurement of the octanol extraction ratio. The dynamic images were weighted and integrated so that the look-up table procedures yielded values of CBF and distribution volume (V_d) simultaneously. **Results:** Calculated values for CBF and V_d were consistent with those determined by nonlinear least squares fitting [CBF: $Y = 1.03X - 0.30$ (ml/100 ml/min), $r = 0.998$, $p < 0.001$; V_d: $Y = 0.99X - 0.11$ (ml/ml), $r = 0.99$, $p < 0.001$] and calculated CBF correlated significantly with CBF measured by PET [$Y = 0.85X - 0.15$ (ml/100 ml/min), $r = 0.92$, $p < 0.001$]. **Conclusion:** This technique is valid for estimating CBF.

Key Words: iodine-123-iodoamphetamine; single-photon emission computed tomography; cerebral blood flow; weighted integration technique

J Nucl Med 1995; 36:531–536

Iodine-123-N-isopropyl-p-iodoamphetamine (IMP) has been used as a cerebral blood flow (CBF) tracer for SPECT due to its large first-pass extraction fraction and high affinity for the brain (*1,2*). The original method developed to measure CBF was based on a microsphere model (*3*). Several investigators have subsequently demonstrated, however, that significant clearance from the brain causes changes in the IMP distribution (*4,5*) and underestimation of CBF values, particularly with a prolonged scan initiation (*6–8*).

Although a two-compartment model has been suggested, it is not conventional because it requires a nonlinear least squares fitting technique which needs a great deal of time for calculation and is not suitable for calculating CBF on a pixel-by-pixel basis. Alpert et al. developed an alternative approach of analyzing dynamic emission and input function datasets (*9*). This entails weighting and integrating the original tissue image data to linearize the model equation defined by the two-compartment model (*10–14*) followed by rapid generation of functional values for CBF and distribution volume with look-up table procedures. The purpose of the present study was to develop a technique for rapid calculation of CBF and distribution volume for IMP using a two-compartment model and a weighted integration technique linked with a look-up table procedure.

MATERIALS AND METHODS

Theory

A two-compartment model (Fig. 1) was used to analyze IMP kinetics in the brain as previously reported (*6,7*):

$$\frac{dC_b(t)}{dt} = K_1 \cdot C_a(t) - k_2 \cdot C_b(t), \qquad \text{Eq. 1}$$

where $C_b(t)$ is the concentration of radioactivity in the brain; $C_a(t)$ is the arterial input function; K_1 is the influx rate constant (ml/ml/min); and k_2 is the efflux rate constant (1/min). In this study, we assumed the first-pass extraction fraction of IMP (E) to be unity (*1,2*) and therefore K_1 equals CBF.

The ratio of K_1 to k_2 is called the distribution volume of IMP in

Received Jul. 1, 1994; revision accepted Sept. 20, 1994.

For correspondence or reprints contact: Hiroshi Ito, MD, Dept. of Nuclear Medicine and Radiology, Division of Brain Sciences, Institute of Development, Aging and Cancer, Tohoku University 4-1 Seiryo-Machi, Aoba-Ku, Sendai City, Japan 980.

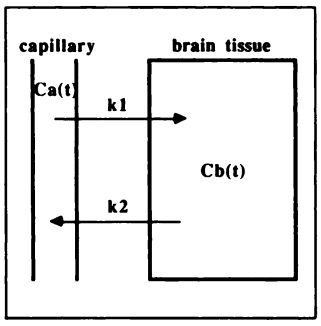

FIGURE 1. A schematic of IMP kinetics in the brain. k_1 and K_2 denote influx and efflux rate constants, respectively. CBF corresponds to K_1 and the distribution volume (V_d) corresponds to the ratio of K_1/K_2.

the brain (V_d (ml/ml)). The V_d is proportional to the brain-blood partition coefficient of IMP, affected by the systematic underestimation of radioactivity concentration due to the limited spatial resolution of the SPECT scanner (*15*).

Solving Equation 1 provides:

$$C_b(t) = K_1 \cdot C_a(t) \otimes e^{-k_2 \cdot t}, \quad \text{Eq. 2}$$

where $\otimes$ denotes the convolution integral.

Multiplying by two independent weight functions and integrating for a time period [0, T] yields the following two equations:

$$\int_0^T W_1(t) \cdot C_b(t)\, dt = K_1 \cdot \int_0^T W_1(t) \cdot C_a(t) \otimes e^{-k_2 \cdot t}\, dt, \quad \text{Eq. 3a}$$

$$\int_0^T W_2(t) \cdot C_b(t)\, dt = K_1 \cdot \int_0^T W_2(t) \cdot C_a(t) \otimes e^{-k_2 \cdot t}\, dt, \quad \text{Eq. 3b}$$

where the integration interval was 1 sec. $W_1(t)$ and $W_2(t)$ are independent weight functions. In this study, the following two weight functions were used as suggested by Alpert et al. (*9*):

$$W_1(t) = 1,\ W_2(t) = t,$$

where $W_2(t)$ i.e., t, corresponds the mean time of the integration time interval. Calculating the ratio of Equation 3A to 3B gives:

$$\frac{\int_0^T W_1(t) \cdot C_b(t)\, dt}{\int_0^T W_2(t) \cdot C_b(t)\, dt} = \frac{\int_0^T W_1(t) \cdot C_a(t) \otimes e^{-k_2 \cdot t}\, dt}{\int_0^T W_2(t) \cdot C_a(t) \otimes e^{-k_2 \cdot t}\, dt} \quad \text{Eq. 4}$$

For a given input function, $C_a(t)$, the ratio of integrals on the right side of Equation 4 can be considered to tabulate as a function of k_2. Then, for a given ratio of integrals of the tissue concentrations, a look-up table procedure provides a corresponding k_2 value. By inserting this k_2 value into Equation 3A or 3B, a K_1 value that corresponds to CBF can be calculated (*9*).

Subjects

Studies were performed on five subjects, including four patients with cerebral infarction and one healthy volunteer (age 62.4 ± 21.2 yr; mean ± s.d.) (Table 1). Informed consent was obtained from all subjects. The project was approved by the PET Research Committee.

SPECT

Dynamic SPECT imaging was initiated after intravenous injection of 222 MBq of IMP for 1 min. The dynamic scan sequence consisted of ten 2-min scans, ten 4-min scans and three 10-min scans. The arterial input function was measured by frequent blood sampling from the radial artery and by determining radioactivity concentrations of octanol-extracted components. Arterial blood gas analyses were performed at 5 min, 10 min, 20 min and 60 min after initiation of the SPECT scan (Table 1). The SPECT scanner used was a HEADTOME-II (Shimadzu Corp. Kyoto, Japan) (*16*), which has three detector rings with 64 NaI rectangular detectors. In-plane resolution was 12 mm FWHM, and the slice thickness was 17 mm FWHM at the center of the field of view. Image slices were obtained at 7, 42 and 77 mm above the orbito-meatal (OM) line. Attenuation correction was made numerically by assuming the object shape to be an ellipse and the attenuation coefficient to be uniform. A cross-calibration scan was obtained using a 16-cm inner diameter cylindrical uniform phantom for calibrating sensitivity between the SPECT scanner and the well counter system.

PET

PET studies were performed for all subjects on the same day as the SPECT studies. As with the SPECT study, image slices were parallel to the OM line. The PET scanner used was a HEAD-

TABLE 1
Subject Profiles

Subject no.	Age	Sex	Diagnosis	Heart disease	Smoking	$PaCO_2$ (mmHg) SPECT†	$PaCO_2$ (mmHg) PET‡
1	63	M	Chronic cerebral infarction	None	+	40.3	40.7
2	79	M	Acute cerebral infarction	None	+	38.4	39.4
3	74	F	Acute cerebral infarction	MR*, chronic heart failure	–	39.7	37.1
4	70	M	Chronic cerebral infarction	None	+	40.5	40.1
5	26	M	Healthy volunteer	None	+	42.2	42.9

*MR; mitral regurgitation.
†Average of four measurements.
‡Average of two measurements.
No subject had lung disease.

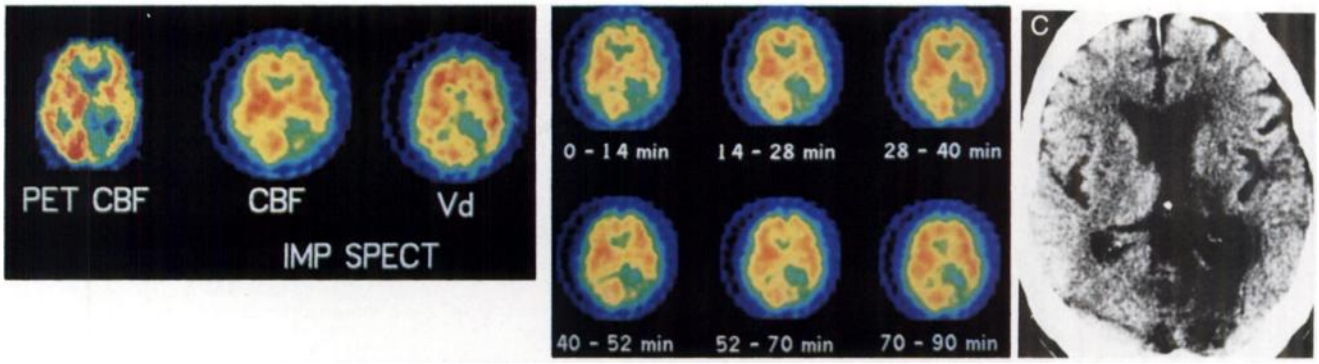

FIGURE 2. (A) Comparison of a ^{15}O-water PET CBF image with CBF and V_d images from a patient with chronic cerebral infarction (Subject 4). The two CBF images are similar, and low V_d values are observed in the infarcted region in the left posterior cerebral artery territory. A discrepancy between the CBF and V_d result is observed around the region, i.e., the size of the defect is smaller in the V_d case. (B) Images obtained by adding frames of IMP dynamic SPECT for a patient with chronic cerebral infarction. The early image (0–14 min) agrees well with the CBF image technique, and a delay in scanning is associated with a distribution closer to the V_d image (Fig. 2A). (C) An x-ray CT image from the same patient. A low density area, i.e., the infarcted region, is observed in the left posterior cerebral artery territory.

TOME-IV (Shimadzu Corp. Kyoto, Japan) (*17*), which provides 14-slice images. In-plane resolution was 8 mm FWHM, and the slice thickness was 9 mm FWHM at the center of the field of view. Following bolus intravenous injection of 555 MBq of ^{15}O-water, a 90-sec scan was obtained. The arterial input function was determined by continuous measurement of whole blood radioactivity using a beta probe. Delay and dispersion occurring in the beta detector system and in the internal-arterial line were corrected according to a previously reported method (*18,19*). The CBF images were calculated autoradiographically (*20–23*). In addition, two blood samples were taken at the beginning and at the end of scanning to measure arterial CO_2 gaseous pressure (Table 1).

Image Analysis

All reconstructed images were transferred to a UNIX workstation (TITAN-750, Kubota Computer Corp., Yamanashi, Japan) for further analysis. Regions of interest (ROIs) were located in the cerebellum and cerebral cortex, including territories of the anterior cerebral artery, middle cerebral artery anterior trunk, middle cerebral artery middle trunk, middle cerebral artery posterior trunk and posterior cerebral artery. ROIs were circles with a 32 mm diameter for the cerebellum and ellipses with a short-axis of 16 mm and long-axes of 16–64 mm for the cerebral cortex. ROIs were also located on the PET images using the same criteria.

RESULTS

The time taken to calculate one slice functional images by the present technique was about 3 min when the integration interval was 1 sec. This calculation speed is about ten times faster than that with conventional analysis, i.e., a nonlinear least squares fitting technique.

Figure 2A shows typical examples of CBF and V_d images calculated by the present technique with IMP-SPECT for a patient with chronic cerebral infarction (Subject 4, Table 1). Regional distribution of CBF calculated by the present technique proved similar to that from the PET technique, with nonuniform V_d values in the brain. It can be seen that the early image (0–14 min) is in good agreement with the CBF image, and that later images come closer to the V_d image (Fig. 2B). Low V_d values were observed in infarcted regions as determined by x-ray CT images (Fig. 2C), and defect sizes in V_d were found to be smaller than for CBF and were consistent with sizes of infarcted regions on x-ray CT images.

Figure 3 summarizes results for the correlation between CBF values obtained by PET and those gained by the present technique using IMP. A good correlation was obtained ($Y = 0.85X - 0.15$ (ml/100ml/min), $r = 0.92$, $p < 0.001$).

CBF values evaluated by the IMP technique were consistent with those from the nonlinear least squares fitting (*24*) for the IMP dynamic SPECT data (Fig. 4) ($Y = 1.03X - 0.30$ (ml/100ml/min), $r = 0.998$, $p < 0.001$). V_d values evaluated by the present technique using IMP were also consistent with

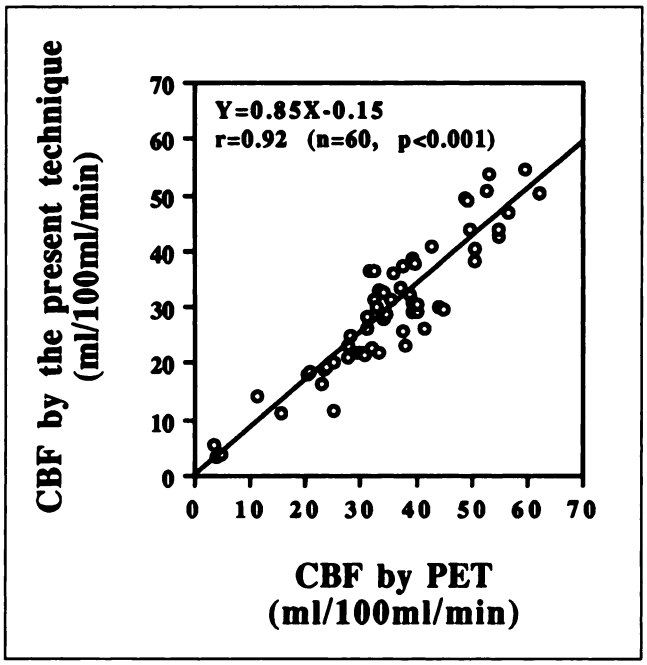

FIGURE 3. Correlation between CBF values obtained by the ^{15}O-water PET and present techniques. A good correlation is observed between the two methods.

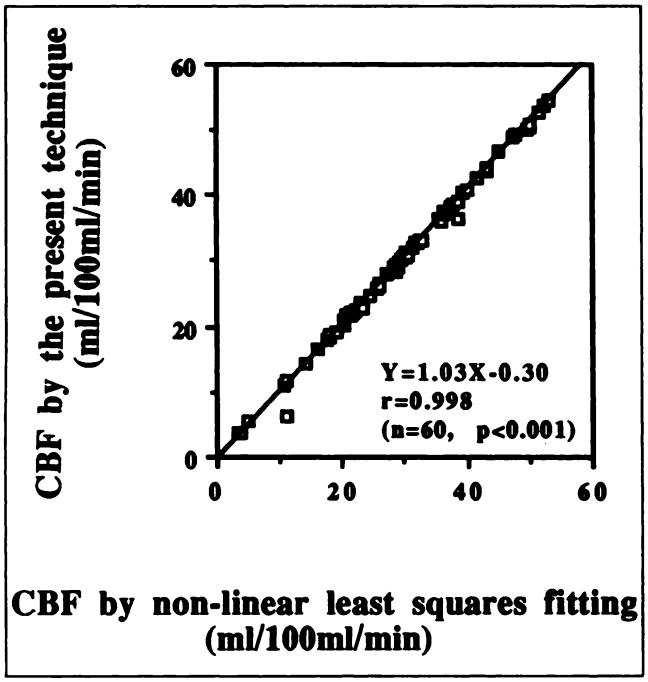

FIGURE 4. Correlation between CBF values evaluated by nonlinear least squares fitting using dynamic SPECT data and those generated by the present technique. The data are very consistent for the two methods.

those generated by the nonlinear least-squares fitting technique for the IMP dynamic SPECT data (Fig. 5) ($Y = 0.99X + 0.11$ (ml/ml), $r = 0.99$, $p < 0.001$).

Figure 6 shows a comparison of V_d values in x-ray CT images of normal density regions ($V_d = 30.3 \pm 8.19$ (ml/ml)) with those in infarcted regions ($V_d = 14.1 \pm 4.16$ (ml/ml)), V_d being significantly reduced in the latter ($p < 0.001$).

DISCUSSION

Technique Validation

The early IMP-SPECT scan images are similar to the CBF images; they later became similar to the V_d images (Fig. 2A, 2B). It has been reported that prolonged SPECT scan initiation causes underestimation of CBF values calculated by microsphere model analysis (*7,8*). These data clearly indicate significant clearance of IMP from the brain, therefore requiring use of a two-compartment model. Such two-compartment model analysis for IMP kinetics in the brain has actually been reported by several investigators (*6–8*).

A combined weighted integration and look-up table procedure was earlier described for rapid calculation of CBF images with ^{15}O-water PET (*9*). The present study confirmed that the calculation speed is sufficiently fast for generation of functional maps of CBF and V_d, the gained values being consistent with those from the nonlinear least squares fitting using IMP dynamic SPECT. This adds support to the applicability of weighted integration and look-up table procedures for analysis of IMP kinetics in the brain,

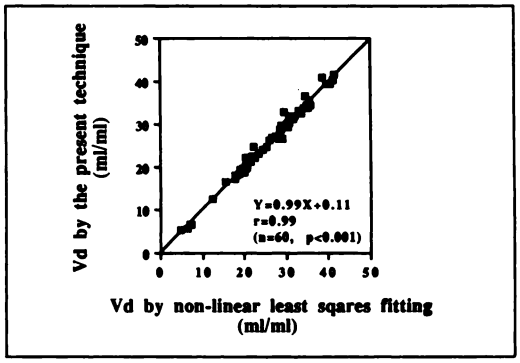

FIGURE 5. Correlation between V_d values evaluated by the nonlinear least-squares fitting technique using the dynamic SPECT data and those generated by the present technique. The data are consistent for the two methods.

which is more advantageous than time-consuming conventional analysis techniques, i.e., nonlinear least squares fitting.

Systematic underestimation of CBF values, as compared with the PET technique (Fig. 3), is probably due to the poorer spatial resolution of SPECT. Another reason is the limited first-pass across the capillary membrane. Values for the first-pass extraction fraction of IMP were previously reported as 0.92–0.74 for a CBF range of 33.0–66.0 ml/100 g/min (*3*), 0.90–0.89 for a CBF range of 54.0–56.0 ml/100 g/min (*25*) and 0.85 for a CBF of 50.0 ml/100 g/min (*26*).

Distribution Volume of IMP

Distribution volume of IMP (V_d) was not found to be uniform in the brain (Fig. 2A). One reason for this might be that the physiological brain-blood partition coefficient of IMP is not a constant. Another possibility is that the fraction of the brain tissue mass per given ROI demonstrated variation due to the limited spatial resolution of the SPECT scanner.

Lear et al. reported that the distribution volume of IMP is an indicator of IMP retention in the brain (*27*), although the physiological background remains to be clearly explained. There have been several reports concerning the

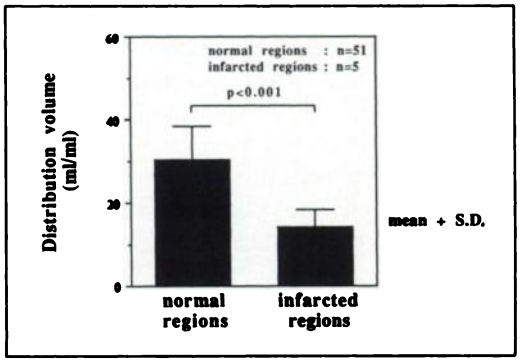

FIGURE 6. Comparison of V_d values in normal regions with those in infarcted regions, as determined by x-ray CT. The difference is highly significant.

significance of IMP accumulation in the brain, indicating the involvement of amine metabolism (*2*), oxygen metabolism (*28*) or functions other than cerebral blood flow (*25*). In this study, significantly lowered V_d values were observed in regions determined to be infarcted by x-ray CT (Fig. 6). It should be noted that a discrepancy was observed between CBF and V_d around infarcted cerebral regions, i.e., defects in V_d were smaller than in CBF (Fig. 2A), but were consistent with the sizes of infarcted regions on x-ray CT images (Fig. 2C). It was previously reported that IMP hypofixation of the peri-infarct area appearing as normal density on x-ray CT was observed on the early image and had disappeared on delayed image (*29,30*). In this study, it was also observed that the early image was in good agreement with the CBF image, and that later images become closer to the V_d image (Fig. 2B).

It has been reported that IMP is metabolized to lipophilic and water-soluble metabolites, i.e., p-iodoamphetamine (PIA) and p-iodobenzoic acid (PIB), respectively, in the brain and other organs (*31*). The water-soluble metabolite cannot be transported across the intact blood-brain barrier. On the other hand, it has also been reported that PIA kinetics are not significantly different from those of IMP (*32*). Therefore the radioactivity of plasma octanol extracted components in this study, including IMP and PIA, was used as an arterial input function. Matsuda et al. (*33*) reported that PIA was the only metabolite observed in acute ischemic brain. In some pathological conditions, however, in which the blood-brain barrier is destructed, e.g., subacute ischemic brain, water-soluble metabolites (PIB) may be transported across the blood-brain barrier and modify IMP distribution in the brain (*30,33*). Further studies are required to clarify the significance of IMP distribution in the brain, especially in pathological conditions.

CONCLUSION

The present approach to calculating functional maps for CBF and V_d using weighted integration and look-up table procedures required about 3 min to calculate one CBF image slice. If the weighted integration process could be simultaneously performed with SPECT data acquisition using an electronic circuit, dynamic SPECT imaging needing larger memory capacity could be discontinued and a more rapid calculation of CBF would be possible (*34*).

ACKNOWLEDGMENTS

The authors thank the staff of the Research Institute for Brain and Blood Vessels, Akita. This work was previously presented at the 39th Annual Meeting of the Society of Nuclear Medicine, Los Angeles, CA, 1992. This study was supported in part by a Research Grant for Aging and Health from the Japanese Ministry of Health and Welfare and a Grant-in-Aid for Scientific Research (03670554) from the Japanese Ministry of Education, Science and Culture.

REFERENCES

1. Winchell HS, Baldwin RM, Lin TH. Development of ^{123}I-labeled amines for brain studies: localization of ^{123}I-iodophenylalkyl amines in rat brain. *J Nucl Med* 1980;21:940–946.
2. Winchell HS, Horst WD, Braun L, Oldendorf WH, Hattner R, Parker H. N-isopropyl-[^{123}I] p-iodoamphetamine: single-pass brain uptake and washout; binding to brain synaptosomes; and localization in dog and monkey brain. *J Nucl Med* 1980;21:947–952.
3. Kuhl DE, Barrio JR, Huang SC, et al. Quantifying local cerebral blood flow by N-isopropyl-p-[^{123}I]iodoamphetamine (IMP) tomography. *J Nucl Med* 1982;23:196–203.
4. Creutzig H, Schober O, Gielow P, et al. Cerebral dynamics of N-isopropyl-(123I)p-iodoamphetamine. *J Nucl Med* 1986;27:178–183.
5. Nishizawa S, Tanada S, Yonekura Y, et al. Regional dynamics of N-isopropyl-(123I)p-iodoamphetamine in human brain. *J Nucl Med* 1989;30:150–156.
6. Greenberg JH, Kushner M, Rango M, Alavi A, Reivich M. Validation studies of iodine-123-iodoamphetamine as a cerebral blood flow tracer using emission tomography. *J Nucl Med* 1990;31:1364–1369.
7. Murase K, Tanada S, Mogami H, et al. Validation of microsphere model in cerebral blood flow measurement using N-isopropyl-p-(^{123}I) iodoamphetamine. *Med Phys* 1990;17:79–83.
8. Yonekura Y, Nishizawa S, Mukai T, et al. Functional mapping of flow and back-diffusion rate of N-isopropyl-p-iodoamphetamine in human brain. *J Nucl Med* 1993;34:839–844.
9. Alpert NM, Eriksson L, Chang JY, et al. Strategy for the measurement of regional cerebral blood flow using short-lived tracers and emission tomography. *J Cereb Blood Flow Metab* 1984;4:28–34.
10. Huang SC, Carson RE, Phelps ME. Measurement of local blood flow and distribution volume with short-lived isotopes: a general input technique. *J Cereb Blood Flow Metab* 1982;2:99–108.
11. Huang SC, Carson RE, Hoffman EJ, et al. Quantitative measurement of local cerebral blood flow in humans by positron computed tomography and ^{15}O-water. *J Cereb Blood Flow Metab* 1983;3:141–153.
12. Koeppe RA, Holden JE, Raymond W. Performance comparison of parameter estimation techniques for the quantitation of local cerebral blood flow by dynamic positron computed tomography. *J Cereb Blood Flow Metab* 1985;5:224–234.
13. Carson RE, Huang SC. Error analysis of the integrated projection technique (IP) and the weighted integration method (WI) for measurement of local cerebral blood flow (LCBF) with positron emission tomography (PET) [Abstract]. *J Nucl Med* 1984;25:P88.
14. Carson RE, Huang SC, Green MV. Weighted integration method for local cerebral blood flow measurements with positron emission tomography. *J Cereb Blood Flow Metab* 1986;6:245–258.
15. Iida H, Kanno I, Miura S, Murakami M, Takahashi K, Uemura K. A determination of the regional brain/blood partition coefficient of water using dynamic positron emission tomography. *J Cereb Blood Flow Metab* 1989; 9:874–885.
16. Kanno I, Uemura K, Miura S, Miura Y. HEADTOME: a hybrid emission tomography for single photon and positron emission imaging of the brain. *J Comput Assist Tomogr* 1981;5:216–226.
17. Iida H, Miura S, Kanno I, et al. Design and evaluation of HEADTOME-IV, a whole-body positron emission tomograph. *IEEE* 1989;36:1006–1010.
18. Iida H, Kanno I, Miura S, Murakami M, Takahashi K, Uemura K. Error analysis of a quantitative cerebral blood flow measurement using $H_2{}^{15}O$ autoradiography and positron emission tomography, with respect to the dispersion of the input function. *J Cereb Blood Flow Metab* 1986;6:536–545.
19. Iida H, Higano S, Tomura N, et al. Evaluation of regional differences of tracer appearance time in cerebral tissues using [^{15}O]water and dynamic positron emission tomography. *J Cereb Blood Flow Metab* 1988;8:285–288.
20. Herscovitch P, Markham J, Raichle ME. Brain blood flow measured with intravenous $H_2{}^{15}O$. I. Theory and error analysis. *J Nucl Med* 1983;24:782–789.
21. Raichle ME, Martin WRW, Herscovitch P, Mintun MA, Markham J. Brain blood flow measured with intravenous $H_2{}^{15}O$. II. Implementation and validation. *J Nucl Med* 1983;24:790–798.
22. Kanno I, Iida H, Miura S, et al. A system for cerebral blood flow measurement using an $H_2{}^{15}O$ autoradiographic method and positron emission tomography. *J Cereb Blood Flow Metab* 1987;7:143–153.
23. Iida H, Kanno I, Miura S. Rapid measurement of cerebral blood flow with positron emission tomography. In: *Exploring brain function anatomy with positron tomography*. New York: Wiley-Interscience Publication; 1991:23–42.

24. Marquardt DW. An algorithm for least-squares estimation of nonlinear parameters. *J Soc Indust Appl Math* 1963;11:431–441.
25. Lassen NA, Henriksen L, Holm S, Barry DI, Paulson OB, Vorstrup S. Cerebral blood-flow tomography: xenon-133 compared with isopropyl-amphetamine-iodine-123: concise communication. *J Nucl Med* 1983;24:17–21.
26. Murase K, Tanada S, Inoue T, et al. Measurement of the blood-brain barrier permeability of ^{123}I-IMP, ^{99m}Tc-HMPAO and ^{99m}Tc-ECD in the human brain using compartment model analysis and dynamic SPECT [Abstract]. *J Nucl Med* 1991;32:P911.
27. Lear JL, Ackermann RF, Kameyama M, Kuhl DE. Evaluation of [^{123}I]isopropyliodoamphetamine as a tracer for local cerebral blood flow using direct autoradiographic comparison. *J Cereb Blood Flow Metab* 1982;2:179–185.
28. Yonekura Y, Tanada S, Senda M, Saji H, Torizuka K. Regional distribution of N-isopropyl-p-(^{123}I)iodoamphetamine in cerebrovascular disease compared with regional cerebral blood flow and oxygen metabolism [Abstract]. *J Nucl Med* 1985;26:P25.
29. Raynaud C, Rancurel G, Samson Y, et al. Pathophysiological study of chronic infarcts with ^{123}I-isopropyl-iodoamphetamine (IMP): the importance of peri-infarct area. *Stroke* 1987;18:21–29.
30. Raynaud C, Rancurel G, Tzourio N, et al. SPECT analysis of recent cerebral infarction. *Stroke* 1989;20:192–204.
31. Baldwin RM, Wu JL. In vivo chemistry of iofetamine HCl iodine-123 (IMP). *J Nucl Med* 1988;29:122–124.
32. Rapin JR, Le Poncin-Lafitte M, Duterte D, Rips R, Morier E, Lassen NA. Iodoamphetamine as a new tracer for local cerebral blood flow in the rats: comparison with isopropyliodoamphetamine. *J Cereb Blood Flow Metab* 1984;4:270–274.
33. Matsuda H, Tuji S, Oba H, et al. Autoradiographic analysis of iodoamphetamine redistribution in experimental brain ischemia. *J Nucl Med* 1990;31:660–667.
34. Iida H, Kanno I, Miura S, Murakami M, Takahashi K, Uemura K. A new PET system for three-dimensional and dynamic imaging and for rapid calculation of rate-constant images. *J Cereb Blood Flow Metab* 1989;9(suppl 1):S416.

Scatter

(Continued from page 5A)

I doubt that many battles have been won with the slogans "the future is bleak" and "the outlook is grim." This should not be construed, however, to suggest that all that is needed is a winning slogan. A program must be consistent with the available resources. It must support the belief that the battle can be won, even if resources are limited. Mutual respect, credibility and integrity in responding to queries about the availability of resources would be more effective toward making the lonely soldier standing guard in the cold night believe that the dawn will come, bringing with it the warmth and light of the sun.

Stanley J. Goldsmith, MD
Editor-in-Chief, The Journal of Nuclear Medicine